

# FIELD EMISSION FROM TRIODE FIELD EMITTER WITH PLANAR CARBON-NANOPARTICLE CATHODE

**Kyung Ho Park, Woo jong Seo, Soonil Lee, and Ken Ha Koh**

**Dept. of Molecular Science and Technology, Ajou University, Suwon 442-749, Korea  
Information Display Research Institute, Ajou University, Suwon 442-749, Korea**

## **Abstract**

*Triode field emitters with planar-carbon-nanoparticle (CNP) cathodes were successfully fabricated using the conventional photolithography and the hot-filament chemical vapor deposition. Electron emission from a CNP triode emitter with a 12- $\mu$ m-diameter gate hole started at the gate voltage of 45 V, and the anode current reached the level of  $\sim$ 120 nA at the gate voltage of 60 V, respectively. For the quantitative analysis of the Fowler-Nordheim (F-N) type emission from a CNP triode emitter, we carried out 2-dimensional numerical calculation of electrostatic potential using the finite element method. As it turned out, a radial variation of electric field was very important to account for the emission from a planar emitting layer. By assuming the graphitic work function of 5 eV for CNPs, we were able to extract a consistent set of F-N parameters, together with the radial position of emitting sites.*

## **1. Introduction**

There were many reports regarding the excellent electron emission in a diode configuration from various carbon films. However, not many groups succeeded in fabricating triode emitters with carbon cathodes. The fabrication of triode-type emitters is essential from the application point of view; for example, low driving voltage, high resolution and full gray-scale imaging become possible in triode emitters.

Carbon nanotubes emerged as the promising electron emitters. However, as it turned out, it was particularly hard to fabricate triodes with normal gate structure using carbon-nanotube cathode layers, and only few groups succeed in demonstrating gate-controlled emission from nanotube-cathode triodes [1-3]. This difficulty arose mainly from the peculiar structural trait of nanotubes. They were typically long and very flexible, and therefore, susceptible to cathode-gate short or to a huge gate current. To circumvent these problems, Samsung used either screen-printing method with very large gate holes or

placed gate electrodes underneath cathode layers [4,5], both of which are not ideal for display application.

Very recently, the emission from the triode structure with a cathode film of thin nanocrystalline graphites [NCG], which were intrinsically free from the above problems of nanotubes, was reported [6]. However, NCG triode also had some shortcomings; the deposition temperature was high, 900°C, and the deposition was not selective so that NCG formed not only at the bottom of gate holes but also on gate electrodes. Previously, we reported the excellent electron emission from similar carbon films [7,8]. It is worth emphasizing that in addition to the excellent emission properties, our carbon-nanoparticle (CNP) films had the advantage of selective growth, which became the corner stone of our triode fabrication process.

## **2. Experimental**

Gated planar CNP field emitters with the schematic structure of Fig. 1(a) were fabricated on steam-oxidized silicon substrates. At first, 100-nm thick chrome cathode lines and 60-nm thick NiFe-catalyst layers were deposited in succession by magnetron sputtering. Second, 1.5- $\mu$ m-thick SiO<sub>2</sub> gate-insulator layers were deposited using the chemical vapor deposition (CVD), and then 200-nm thick chrome gates were deposited by sputtering. Next, gate holes were defined using the conventional photolithography, and the gate insulators were wet-etched to expose the catalyst layers through the gate holes. Finally, the hot filament CVD (HFCVD) was carried out to form CNP cathodes inside the gate holes at the deposition temperature of 680°C using the mixtures of methane and hydrogen; HFCVD conditions were similar to those that we used previously to produce large area diode CNP field emitters [7].

## **3. Results and discussion**

Figure 1(b) is typical scanning electron microscopy

(SEM) images of triode CNP emitters. The plane view on the right proves a successful selective deposition of CNP layers, conformal to the area where the metal catalysts were exposed [8], below the gates. Moreover, the image on the left, which shows the CNP layer near the gate-hole edge in higher magnification, reveals that the CNP layer consisted mostly of carbon nanoparticles of  $100 \pm 15$  nm in diameter. However, there were few irregularly shaped lumps, unlike the cases of large area diode CNP emitters, which, we suspect, could be amorphous carbon phase covering either the clusters of nanoparticles or the residue of gate oxide. Nevertheless, the planar CNP cathode maintained relatively smooth surface, and no trace of long carbon nanotubes was observed.

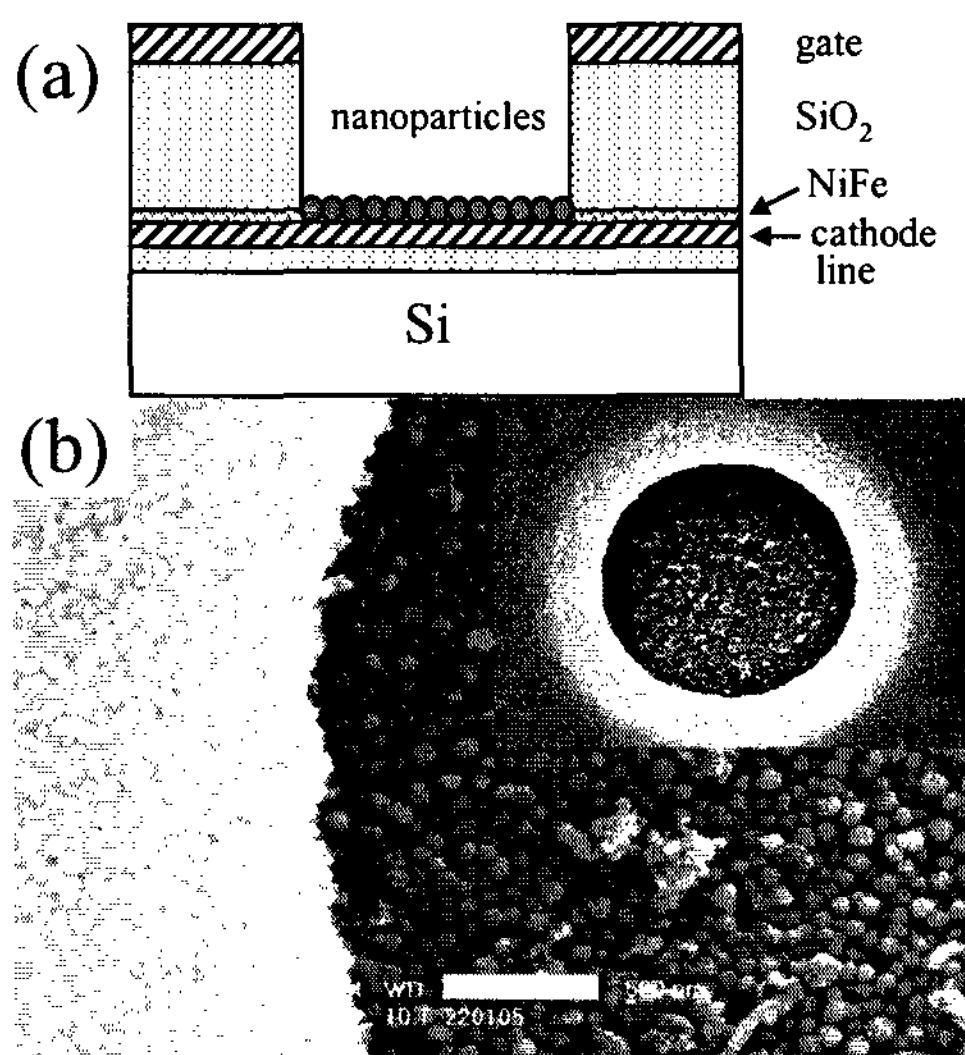


FIG. 1 Schematic structure (a) and typical scanning electron microscopy images (b) of triode CNP emitters. The bar corresponds to 500 nm

Figure 2 shows the gate-voltage dependence of emission images and currents of a single CNP triode emitter with a 12- $\mu\text{m}$ -diameter gate hole. The presented emission results were measured, using a phosphor-coated indium tin oxide (ITO) glass as an anode, at the anode bias of 1000 V with the 110- $\mu\text{m}$  gate-anode separation. The emission started at the gate voltage of 45 V, and the anode current reached the level of  $\sim 120$  nA as the gate voltage was increased to 60 V. The increase in anode current resulted in a concomitant evolution in emission images. Both the brightness and the size of emission spot increased as the gate voltage was increased; images in Fig. 3(a)

correspond to the gate voltage of 50, 54, and 58 V, respectively. It is worth emphasizing that for the increase of emission currents over two orders of magnitude, the ratio between the gate and anode currents remained below  $\sim 4$ . Note that unlike the gate-bias increase, the anode-bias increase did not induce any noticeable change in the emission currents.

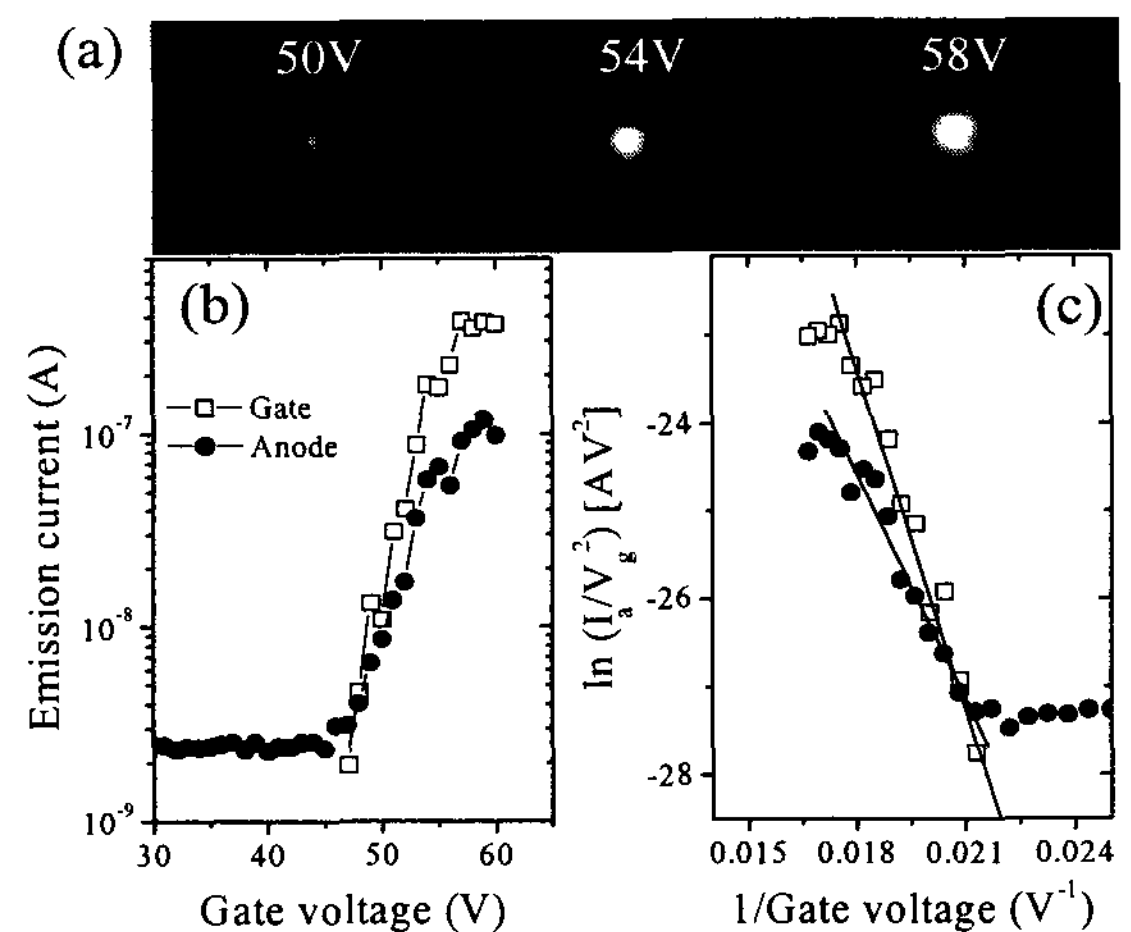


Fig. 2 Gate voltage dependence of emission images (a) and currents (b), and corresponding F-N plots (c) of a single CNP triode emitter with a 12- $\mu\text{m}$ -diameter gate hole.

According to the F-N equation, the emission current  $I(A)$  depends on area  $S(\text{cm}^2)$ , local electric field  $F(V/\text{cm})$ , and work function  $\phi(\text{eV})$  at local sites:  $I = S \cdot A \cdot \exp B$ , where  $A = 1.40 \times 10^{-6} F^2 / \phi$ ,  $B = -6.53 \times 10^7 \phi^{3/2} / F + 9.87 / \sqrt{\phi}$  [9]. Therefore, as long as local field  $F$  is proportional to gate voltage  $V_g$ , plots of  $\ln I / V_g^2$  versus  $1 / V_g$  become linear; the proportionality constant  $\beta_c (\text{cm}^{-1})$  in  $F = \beta_c V_g$  is the field conversion factor. In the diode-emitter case, since the local field  $F$  can be expressed in terms of the bias voltage  $V$  and the field enhancement factor  $\beta$  as  $F = \beta V / d$ , the field conversion factor  $\beta_c$  is equivalent to  $\beta / d$ . However, in the case of triode emitter, the expression for the field conversion factor is generally not as straightforward as their counterpart in the diode cases due to the complex spatial and gate-voltage-dependent variation of local electric field.

For the triode with the structure shown in Fig. 1(a), the electric field has an azimuthal symmetry, and its strength on the surface of the CNP layer depends on the radial distance from the center and the gate voltage:  $E = E(r, V_g; h)$  at the given gate-oxide thickness  $h$ . We carried out 2-dimensional numerical calculation of electrostatic potential using the commercial FEM code ANSYS to determine  $E = E(r, V_g; h)$ . Since ANSYS uses the Laplace's equation as the basis for static-electric-field analysis, the space-charge effect was not taken into account in this simulation,<sup>10</sup> which can be justified unless the emission current becomes exceedingly large at the emitter surface; in the case of our triode the current density remained a few orders of magnitude lower than the threshold value for the space charge effect.<sup>11</sup>

Figure 3(a) shows a typical variation of the electric field for our triode emitter, of which the emission results are shown in Fig. 3. The field variation of  $\sim 16$  and  $\sim 21$  V/ $\mu\text{m}$  was observed over the radial distance of  $6\mu\text{m}$  at  $V_g$  of 45 V and 60 V, respectively. It is worth emphasizing that this radial variation becomes amplified in the local electric field,  $F = \beta E$ , by the field enhancement factor  $\beta$ . Therefore, few emission sites located near the CNP-cathode edge are bound to contribute most of the emission currents due to the  $\exp(-1/F)$ -dependence of the field emission; Fig. 3(b) shows the radial-position dependence of the emission current from the identical emission site. Moreover, the shape of the equipotential lines results in spreading of emitted electrons. Along with the preferential electron emission from the area near the cathode edge, the electron-defocusing effect makes the triode emitter with planar cathodes susceptible to the problem of large gate currents.

Our simulation also showed that at a given radial position  $r_0$  the field strength was proportional to the gate voltage as presented in Fig. 4(a):  $E(r_0, V_g) = \xi(r_0)V_g$ , where  $\xi(r_0)$  is a proportional constant. Therefore, we can express the local field as  $F(r) = \beta E(r, V_g) = \beta \xi(r)V_g = \beta_c(r)V_g$ . Note that  $\xi(r)$ , and consequently  $\beta_c(r)$ , changes rapidly near the cathode edge. Due to this linear dependence of the local field on the gate bias, we were able to determine, while assuming the work function of  $5\text{eV}$ , the field conversion factor  $\beta_c$  and the emission area  $S$  from the slope and the y-axis intercept of the F-N plot of

the total emission current, which is the sum of anode and gate currents:  $\beta_c = 7.1 \times 10^5 \text{ cm}^{-1}$  and  $S = 6.7 \times 10^4 \text{ nm}^2$ . It was interesting to note that even when a work function as low as 4 eV was assumed, we found only a slight change in  $\beta_c$  and  $S$  values.

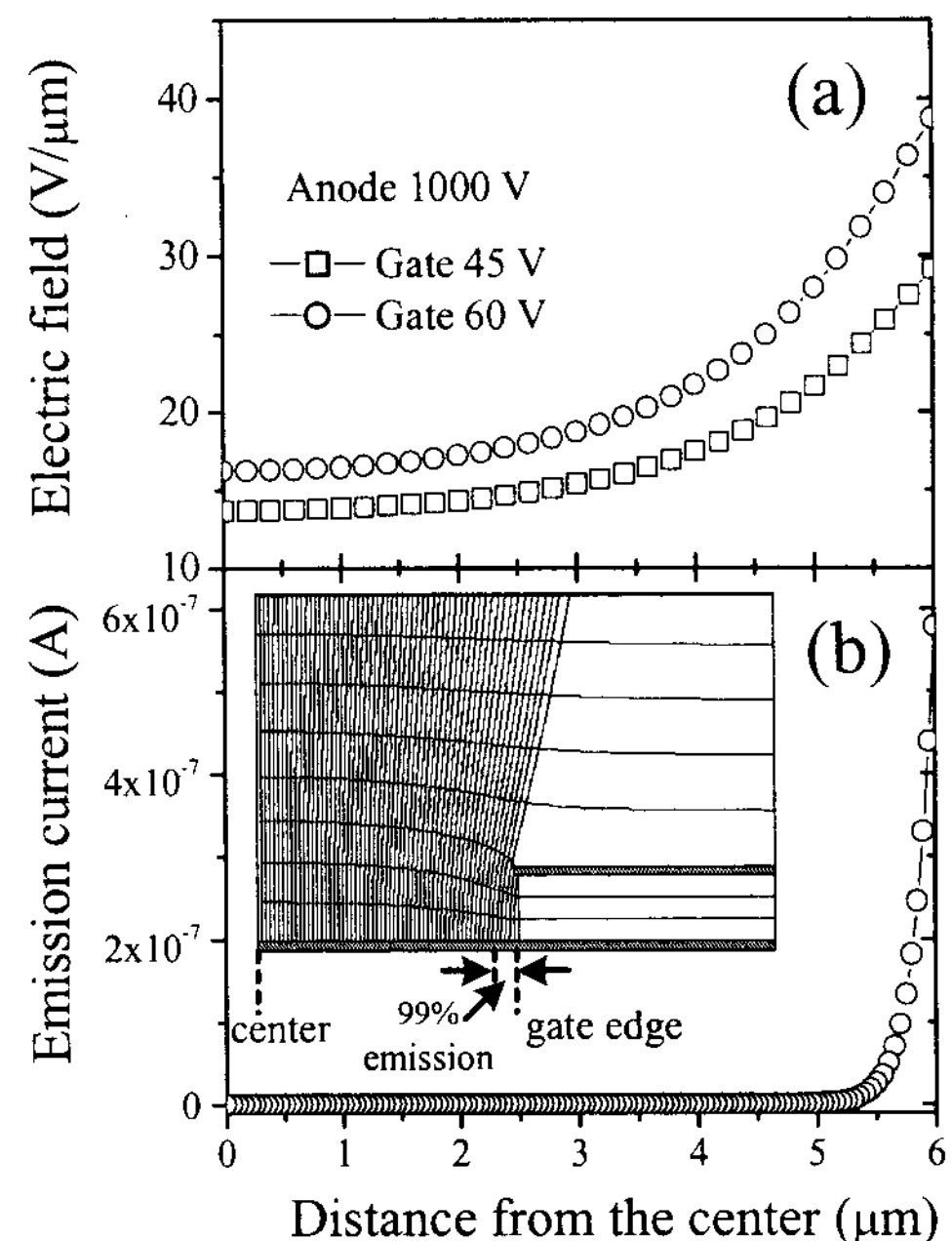


FIG. 3 Radial-position dependence of electric field at the planar cathode surface (a), and the corresponding variation in the emission currents at  $V_g = 60\text{V}$  from the identical emission site of  $\phi = 5.0\text{eV}$ ,  $\beta = 120$ , and  $S = 7.9 \times 10^3 \text{ nm}^2$  (b). The trajectories of emitted electrons are presented in the inset. The area responsible for the 99% of the total emission current is marked with arrows.

If we assume that few CNPs at  $r_0$  were the homogeneous emitters, the total emission area of  $6.7 \times 10^4 \text{ nm}^2$  corresponds to about four active spheres of average diameter of 100 nm (see Fig. 1). In other words, the F-N plot corresponds to the emission current from  $\sim 4$  CNPs, of which the centers were located on the circle of radius  $r_0$ . Within this model, we were able to determine the radial position  $r_0$  of the active CNPs by comparing the simulated  $I(r, V_g)$  with the experimental data; recall the aforementioned  $\exp(-1/F)$ -dependence of the F-N current and the large variation of  $F(r)$  near the cathode edge. The best agreement of simulated total

emission current with the experimental data, shown in Fig. 4(b), was achieved with  $\beta = 120$  and  $r_0 = 5.75 \mu\text{m}$ . It has to be pointed out that with a proper set of  $\beta$  and  $r_0$ , not only the total current but also the ratio between the gate and anode currents,  $I_g / I_a$ , could be well accounted for as shown in Fig. 4(c); to estimate the gate and anode currents we divided a single 100-nm-diameter CNP into 200 subsections and traced emitted electrons from each of these subsections.

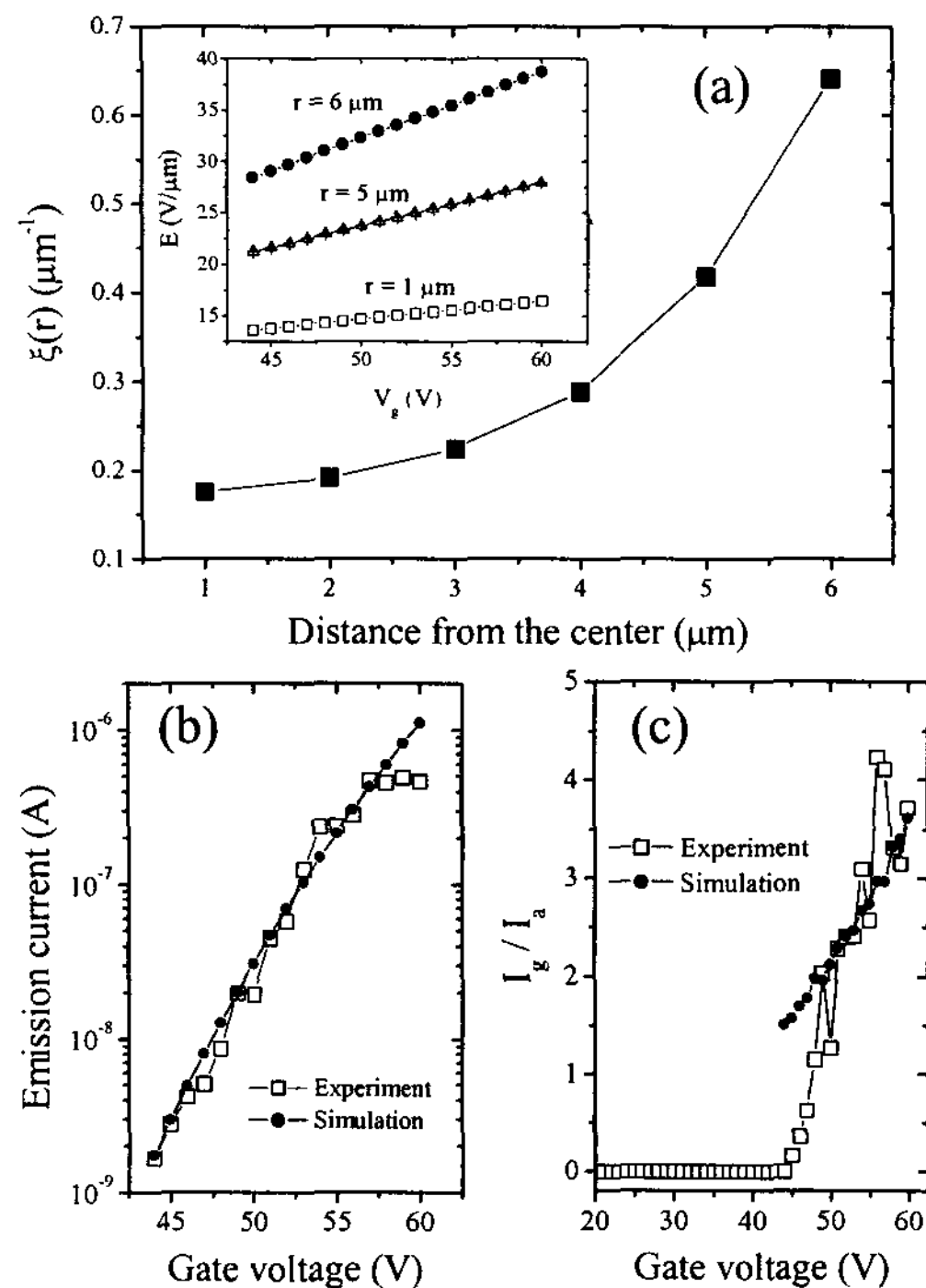


FIG.4 Spatial variation of the gate-bias dependence of the electric-field strength (inset) and radial-position dependence of the ratio between electric field strength and gate bias  $\xi(r)$  (a), comparison between the measured total emission current and the simulated F-N current  $I(r, V_g)$  for  $\beta = 120$  and  $r_0 = 5.75 \mu\text{m}$  (b), and comparison between the simulated and the measured ratio of gate and anode currents,  $I_g / I_a$  (c).

#### 4. Conclusion

We fabricated triode field emitters, which had normal gate structure and planar CNP cathode layers, using the conventional photolithography and HFCVD.

A CNP triode emitter with a 12- $\mu\text{m}$ -diameter gate hole and a 1.5- $\mu\text{m}$ -thick gate-insulator started to emit electrons at the gate voltage of 45 V, and the anode current reached the level of  $\sim 120$  nA at the gate voltage of 60 V. We performed two-dimensional FEM calculation of electrostatic potential and examined a radial variation of electric field on the surface of a planar cathode, which turned out very important for the quantitative account of the observed emission from the CNP triode emitter. Moreover, we extracted a consistent set of Fowler-Nordheim parameters, in addition to presenting the probable radial position of active emitting CNPs.

#### 5. References

- [1] G. Pirio, P. Legagneux, D. Pribat, K. B. K. Teo, M. Chhowalla, G. A. J. Amaratunga, and W. I. Milne, *Nanotechnology* **13**, 1 (2002).
- [2] H. Cheng, K. Chen, W. Hong, F. Tantai, C. Lin, K. Chen, and L. Chen, *Electrochemical Solid-State Lett.* **4**, H15 (2001).
- [3] M. A. Guillorn, A. V. Melechko, V. I. Merkulov, E. D. Ellis, C. L. Britton, and L. R. Baylor, *Appl. Phys. Lett.* **79**, 3506 (2001).
- [4] Y. S. Choi, J. H. Kang, Y. J. Park, W. B. Choi, C. J. Lee, S. H. Jo, C. G. Lee, J. H. You, J. E. Jung, N. S. Lee, and J. M. Kim, *Diamond Relat. Mater.* **10**, 1705 (2001).
- [5] D. S. Chung, S. H. Park, Y. W. Jin, J. E. Jung, Y. J. Park, H. W. Lee, T. Y. Ko, S. Y. Hwang, J. W. Kim, N. H. Kwon, M. H. Yoon, C. G. Lee, J. H. You, N. S. Lee, and J. M. Kim, *Proceedings of the 14th International Vacuum Microelectronics Conference*, UC Davis, USA, (2001) p.179.
- [6] H. Busta, D. Furst, A. T. Rakhimov, V. A. Samorodov, B. V. Seleznev, N. V. Suetin, and A. Silzars, *Appl. Phys. Lett.* **78**, 3418 (2001).
- [7] K. H. Park, S. Choi, K. M. Lee, S. Lee, and K. H. Koh, *J. Vac. Sci. Technol. B* **19**, 958 (2001).
- [8] K. H. Park, K. M. Lee, S. Choi, S. Lee, and K. H. Koh, *J. Vac. Sci. Technol. B* **19**, 946 (2001).
- [9] C. A. Spindt, I. Brodie, L. Humphrey, and E. R. Westerberg, *J. Appl. Phys.* **47**, 5248 (1976).
- [10] P. Kohnke *et al.*, *ANSYS User's Manual*, Swanson Analysis Systems Inc., Houston, USA (1992).
- [11] H. Y. Ahn, "Numerical analysis of field emitters", Ph. D. dissertation, Seoul National University, Korea, (1996).